

Universal Behavior of the Hall Resistivity of Single Crystalline $\text{Bi}_2\text{Sr}_2\text{CaCu}_2\text{O}_x$ in the Thermally Activated Flux Flow Regime

A. V. Samoilov

P. L. Kapitza Institute for Physical Problems, ul. Kosygina 2, Moscow 117334, Russia

(Received 17 July 1992)

The Hall resistivity ρ_H and the longitudinal resistivity ρ of single crystalline $\text{Bi}_2\text{Sr}_2\text{CaCu}_2\text{O}_x$ are measured in the thermally activated flux flow regime. It is shown that ρ_H scales to a universal function of ρ : $\rho_H(T) = A[\rho(T)]^\beta$, where $\beta = 2 \pm 0.1$ and A is a positive and magnetic field independent coefficient for magnetic fields from 1 to 5 T. A resistivity-squared dependence of ρ_H can be explained by the recent theory of Vinokur, Geshkenbein, Feigel'man, and Blatter in terms of weak pinning of a vortex liquid.

PACS numbers: 74.60.Ge, 72.15.Gd, 74.72.Hs

The Hall effect in the mixed state of the high-temperature superconductors (HTSC) remains one of the most intriguing phenomena in the area of the HTSC. In particular, a lot of work [1–5] has been devoted to an unusual sign change of the Hall voltage just below the transition temperature T_c . Chien *et al.* [6] reported detailed measurements of the Hall resistivity in single crystals of $\text{YBa}_2\text{Cu}_3\text{O}_{7-\delta}$ (Y-123) versus magnetic field and discussed the transition from diffusive to activated behavior in the vortex-liquid state. A recent paper by Luo *et al.* [7] has been concerned with the behavior of the Hall resistivity of Y-123 films in the vicinity of the vortex-glass transition [8] at lower temperatures.

For $\text{Bi}_2\text{Sr}_2\text{CaCu}_2\text{O}_x$ (Bi-2212) superconductor there is a remarkable temperature region where dissipation in the mixed state occurs through thermally activated motion of the vortex lines [9]. This region lies between the high-temperature viscous flux flow (VFF) regime and the low-temperature vortex-glass critical behavior. Within the VFF regime the resistivity gradually decreases with temperature, and the vortex state has been suggested to be an unpinned vortex liquid [10]. At lower temperatures the dynamics of the vortex lines is determined by thermal activation over pinning barriers, and the resistivity exponentially depends on temperature. As follows from a SQUID picovoltmetry study on the Bi-2212 single crystals by Safar *et al.* [11], upon a further temperature decrease down to 26–28 K, the crossover from thermal activation to the low-temperature vortex-glass critical behavior occurs in magnetic fields from 2 to 6 T.

Zavaritsky, Samoilov, and Yurgens have observed [12] that in Bi-2212 single crystals the tangent of the Hall angle, $\tan\theta \equiv \rho_H/\rho$, where ρ_H and ρ are the Hall resistivity and the longitudinal resistivity, respectively, tends to zero as the temperature decreases to the thermally assisted flux flow (TAFF) region. As it has been pointed out in Ref. [5], this decrease in the Hall angle occurs because the flux lines are able to creep along the direction of the Lorentz force assisted by the thermal activation. In this Letter we report on the first observation of scaling of the Hall resistivity ρ_H in single crystalline Bi-2212 within the TAFF regime. We have observed a universal behavior of

the Hall resistivity,

$$\rho_H(T) = A[\rho(T)]^\beta, \quad (1)$$

with an exponent $\beta \approx 2$ and a positive magnetic field independent coefficient A over a wide range of magnetic fields (1–5 T). This behavior is distinctly different from previous observations on Bi-2212 single crystals in lower magnetic fields [2] when the Hall voltage is negative.

The high-quality Bi-2212 single crystals were grown as described by Zavaritsky, Samoilov, and Yurgens [13]. The widths of the resistive transition as measured between the 10% and 90% normal-state resistivity levels are about 3 and 4 K for the two samples referred to below as sample 1 and sample 2; the $10^{-2} \mu\Omega \text{ cm}$ resistivity level is reached at 94.0 and 93.1 K for samples 1 and 2, respectively. The sizes of the samples are $2 \times 1 \times 0.01 \text{ mm}^3$ and $1.6 \times 0.7 \times 0.012 \text{ mm}^3$, with the c axis perpendicular to the largest surface of the samples. In this study, the magnetic field is directed parallel to the c axis, $\mathbf{H} \parallel c$. A method of exchanging the voltage and current probes has been used as described in Ref. [12]. Two contacts marked by A and B (see Fig. 2, inset) each covering the square of $l \times d$ (where l and d are the width and thickness of a sample) and two contacts marked by C and D each covering the square of about $0.1 \text{ mm} \times d$ have been made using silver paint deposited on the edges of the samples. The distances between the contacts C and D along the AB line are 1.0 and 0.6 mm for samples 1 and 2, respectively. The samples have been annealed in air at 500°C for 10 h, with subsequent slow cooling to room temperature. After this the copper wires with diameters of $30 \mu\text{m}$ have been attached with conducting glue covering previously painted contacts and small areas on the a - b sides of the samples. No annealing has been done after this stage, so the electric current flows through the edges of a sample. The contact resistances do not exceed 2.5Ω . The dc electric current is used to measure simultaneously the temperature dependences of the a - b plane Hall and longitudinal resistivities at fixed magnetic field. The resistivities are found to be current independent within the range between 0.3 and 8 mA. Most of the data have been obtained at current $I = 3 \text{ mA}$ for sample 1 and at $I = 8 \text{ mA}$ for sample

2. The Hall and longitudinal voltages have been obtained from the odd and even contributions, respectively, under exchanging the roles of the voltage and current leads. At selected temperatures (at 50 K and at temperatures from 60 to 120 K with separation of 15 K) this procedure has been tested to be equivalent within the experimental accuracy to the reversal of the sign of the magnetic field. The odd contribution has been checked to be zero in the absence of an applied magnetic field. The bulk of the data presented are those for sample 1. Data for sample 2 are similar and included in Fig. 2.

No excess dissipation in the form of a "knee," or a "hump," has been observed in the ρ vs T dependences in the mixed state at fields up to maximum available value 5 T, indicating that the c -axis conduction is negligible in our experiments [14]. In the TAFF regime the longitudinal resistivity may be written in the form $\rho = \rho_0 \times \exp(-U_0/T)$, where U_0 is the activation energy. The inset in Fig. 1 shows the Arrhenius plots of the longitudinal resistivity for sample 1 at magnetic fields 1, 3, and 5 T. The slopes of the curves give the activation energies. To examine the form $\rho = \rho_0 \exp(-U_0/T)$, one can plot the $T^2 \partial[\ln(\rho)]/\partial T$ vs T dependences for fixed magnetic fields. In order to compare the data on the activation energies with the data of Fig. 2, in Fig. 1 we plotted $T^2 \partial[\ln(\rho)]/\partial T$ vs ρ . Figure 1 shows that at low resistivities (temperatures) $T^2 \partial[\ln(\rho)]/\partial T$ weakly depends on ρ and starts to increase fast as the resistivities exceed a particular value ρ^* ($\rho^* \approx 15 \mu\Omega \text{ cm}$ for 1 T, $\rho^* \approx 30 \mu\Omega \text{ cm}$ for 3 T, $\rho^* \approx 40 \mu\Omega \text{ cm}$ for 5 T). For resistivities higher than these values, it is meaningless to talk about activated behavior of the resistivity in the form $\rho = \rho_0 \exp(-U_0/$

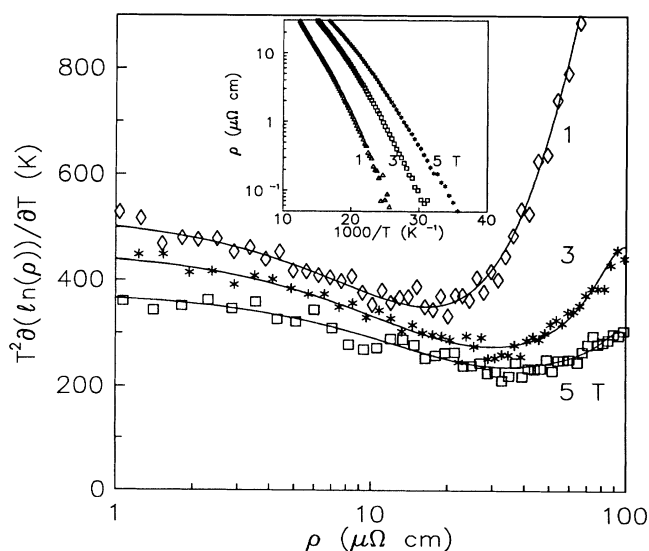


FIG. 1. $T^2 \partial[\ln(\rho)]/\partial T$ vs ρ dependences for sample 1 at magnetic fields 1, 3, and 5 T. Lines are guides for the eye. Inset: The Arrhenius plots of the resistivity for magnetic fields 1, 3, and 5 T.

T). We postulate the crossover from the TAFF regime to the VFF regime to be at the temperature T^* at which $\rho(T^*, H) = \rho^*(H)$. For all magnetic fields ranging from 1 to 5 T, $T^* \approx 65$ –67 K. The difference between the values of ρ^* for sample 2 and those for sample 1 does not exceed 20%.

Figure 2 shows the resistivity dependences of ρ_H for fixed magnetic fields in a log-log scale. The Hall resistivity is positive in the normal state (within the high-resistivity parts of the curves) and proportional to the magnetic field strength. As the temperature decreases below T_c , ρ_H changes sign and becomes negative for all magnetic fields but 5 T (for sample 1). Those parts of the ρ_H vs ρ curves where ρ_H is negative are not shown in the figure. With further temperature (and resistivity) decrease the Hall resistivity starts to increase, passes through a maximum, and finally drops in the low-resistivity parts of the curves.

The striking feature of Fig. 2 is that the low-resistivity parts of the curves scale to the universal power-law dependence given by Eq. (1) with $\beta = 2 \pm 0.1$ and a coefficient A which is approximately magnetic field independent. The higher the magnetic field is, the wider is the region where good scaling can be observed. For a field of 5 T, scaling can be observed over 2 orders of magnitude in the Hall resistivity. Comparing data of Figs. 1

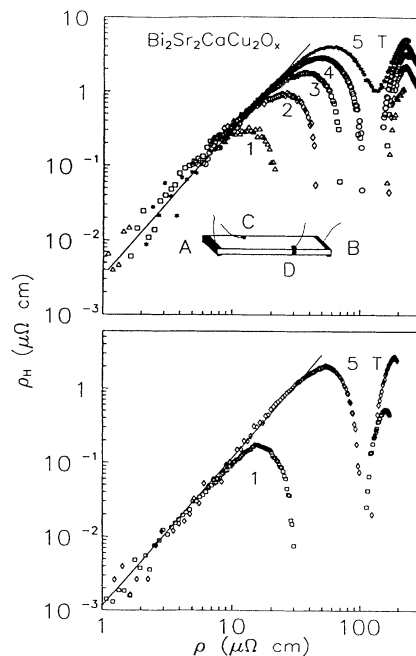


FIG. 2. ρ_H vs ρ dependences at magnetic fields ranging from 1 to 5 T for sample 1 (top) and for sample 2 (bottom). The solid lines represent a fit by the theory of Vinokur *et al.* [15] [Eq. (3)], with $a/H = (7 \pm 2) \times 10^{-10} \text{ kg m}^{-1} \text{ s}^{-1} \text{ T}^{-1}$ (sample 1, top) and $a/H = (2.4 \pm 0.6) \times 10^{-10} \text{ kg m}^{-1} \text{ s}^{-1} \text{ T}^{-1}$ (sample 2, bottom). The inset shows the contact configuration. Dimensions in the direction of the c axis are not on scale.

and 2, one notices that this universal behavior occurs at resistivities slightly below $\rho^*(H)$. On the other hand, as is seen from Fig. 1, $T^2\partial[\ln(\rho)]/\partial T$ does not exhibit a sharp increase with decreasing temperature at low-resistivity parts of the curves, which testifies that the temperatures we are operating at are above the crossover to the vortex-glass critical behavior [11]. Thus, that part of the H vs T diagram where scaling is observed lies entirely within the TAFF region and approximately coincides with it wherever we are able to measure the Hall resistivity.

The explanation of such a scaling has been done in the recent theory of Vinokur, Geshkenbein, Feigel'man, and Blatter [15]. Following them, let us write the equation for the forces acting on the vortices in the absence of pinning,

$$\eta\mathbf{v} + \alpha\mathbf{v} \times \mathbf{n} = \Phi_0\mathbf{j} \times \mathbf{n}, \quad (2)$$

where η is the viscous drag coefficient, α is the Hall drag coefficient, \mathbf{v} is the vortex line velocity, Φ_0 is the flux quantum, and \mathbf{n} is the unit vector in the direction of magnetic field. The term on the right-hand side of Eq. (2) is the Lorentz force acting on the vortex line due to the presence of the transport current.

Vinokur, Geshkenbein, Feigel'man, and Larkin have shown [10] that a vortex liquid can be pinned by weak disorder with an averaged pinning force which can be written in the form $\mathbf{f}_{\text{pin}} = -\gamma\mathbf{v}$, where γ is a coefficient associated with the plastic motion of the vortices and is independent of the vortex line velocity in the linear limit. It then follows that the pinning force renormalizes the first term on the left-hand side of Eq. (2) and does not affect the second, Hall term. Therefore, the expression for the Hall resistivity in terms of ρ is [15]

$$\rho_H = (\alpha/\Phi_0 H)\rho^2, \quad (3)$$

and the coefficient A introduced in Eq. (1) is related to α via $A = \alpha/\Phi_0 H$ if we let β be equal to 2. Comparing the theoretical result with the experimental one presented in Fig. 2, one can make the following conclusions.

(1) With decreasing temperature, the pinning force becomes increasingly important. Within the TAFF regime, $\gamma \gg \eta$ and ρ changes very rapidly in a narrow temperature region. Hence, although both α and ρ are temperature dependent, the main temperature dependent factor is ρ^2 , whereas possible changes of α with temperature are small.

(2) Neglecting the temperature dependence of α over the TAFF region for magnetic fields between 1 and 5 T, one computes $\alpha/H = (7 \pm 2) \times 10^{-10} \text{ kg m}^{-1} \text{ s}^{-1} \text{ T}^{-1}$ and $\alpha/H = (2.4 \pm 0.6) \times 10^{-10} \text{ kg m}^{-1} \text{ s}^{-1} \text{ T}^{-1}$ for samples 1 and 2, respectively, such that ρ_H vs ρ dependence is universal for all magnetic fields. The result that α is proportional to the magnetic field strength is consistent with the Bardeen-Stephen theory [16] in which the Hall effect in the mixed state results as just in the normal state. The

discrepancy in the values of α for the two samples may be thus attributed to the discrepancy in the normal-state resistivities.

(3) The sign of the Hall resistivity is determined by the sign of α . This coefficient is suggested to be strongly temperature dependent in the vicinity of the transition temperature.

(4) The fact that the Hall voltage is positive within the TAFF regime where pinning is mostly important provides an evidence that the sign change of the Hall resistivity near T_c is not related to pinning. Observation of the scaling behavior within the positive Hall resistivities, together with the data of Luo *et al.* [7] on the scaling for the negative Hall resistivities, indicates that the scaling and the sign reversal of ρ_H are decoupled, in agreement with the theory [15].

Previously, Artemenko, Gorlova, and Latyshev [2] observed that ρ and ρ_H of a Bi-2212 single crystal had the same temperature dependence in low magnetic fields, when the Hall voltage is negative everywhere in the mixed state. As this differs from our results for the high field regime, a few comments on the low field behavior are in place. In Fig. 3 we show the temperature dependence of the tangent of the Hall angle $\tan\theta = \rho_H/\rho$ for a small field $H = 0.1$ T. It is easy to see that although $\tan\theta \approx \text{const}$ within a narrow temperature region between 85 and 90 K, there is a clear tendency for $\tan\theta$ to decrease as the temperature decreases below 85 K. The observation of an equal T dependence for both ρ and ρ_H can be explained in a natural way if we assume that the measurements of Ref. [2] have been carried out in the vicinity of the minimum of the $\tan\theta$ vs T curve. The inset in Fig. 3 shows the same data in a log-log plot of $|\rho_H|$ vs ρ . The

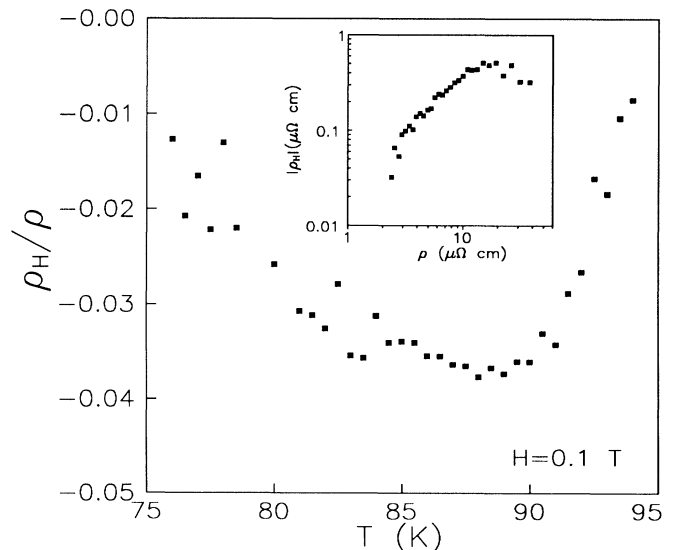


FIG. 3. The temperature dependence of ρ_H/ρ for sample 1 at magnetic field 0.1 T. Inset: $|\rho_H|$ vs ρ dependence for magnetic field 0.1 T.

power-law dependence is questionable here. As the measurements in low fields are carried out in the nearest vicinity of T_c , we believe that α and not ρ provides the main temperature dependent factor.

To summarize, a new universal, approximately resistivity-squared dependence has been found for the Hall resistivity within the TAFF regime. The Hall drag coefficient α is determined to be proportional to magnetic fields ranging from 1 to 5 T, in agreement with the Bardeen-Stephen model, with α/H of the order of $10^{-10} \text{ kgm}^{-1} \text{ s}^{-1} \text{ T}^{-1}$. The observation of positive Hall resistivity within the TAFF regime clearly indicates that pinning is not responsible for the sign change of ρ_H . The experimental results are consistent with the theory of Vinokur, Geshkenbein, Feigel'man, and Blatter and give new insights into the vortex motion in the mixed state of the HTSC.

I gratefully acknowledge stimulating discussions with N. V. Zavaritsky, M. V. Feigel'man, and V. B. Geshkenbein.

-
- [1] M. Galfy and E. Zirgiebl, *Solid State Commun.* **68**, 929 (1988).
 - [2] S. N. Artemenko, I. G. Gorlova, and Y. I. Latyshev, *Pis'ma Zh. Eksp. Teor. Fiz.* **49**, 352 (1989) [*JETP Lett.* **49**, 403 (1989)].
 - [3] Y. Iye, S. Nakamura, and T. Tamegai, *Physica (Amsterdam)* **159C**, 616 (1989).
 - [4] S. J. Hagen, C. J. Lobb, R. L. Greene, M. G. Forrester,

- and J. H. Kang, *Phys. Rev. B* **41**, 11630 (1990).
- [5] Z. D. Wang and C. S. Ting, *Phys. Rev. Lett.* **67**, 3618 (1991).
- [6] T. R. Chien, T. W. Jing, N. P. Ong, and Z. Z. Wang, *Phys. Rev. Lett.* **66**, 3075 (1991).
- [7] J. Luo, T. P. Orlando, J. M. Graybeal, X. D. Wu, and R. Muenchausen, *Phys. Rev. Lett.* **68**, 690 (1992).
- [8] M. P. A. Fisher, *Phys. Rev. Lett.* **62**, 1514 (1989); D. S. Fisher, M. P. A. Fisher, and D. A. Huse, *Phys. Rev. B* **43**, 130 (1991).
- [9] T. T. M. Palstra, B. Batlogg, L. F. Schneemeyer, and J. V. Waszczak, *Phys. Rev. Lett.* **61**, 1662 (1988).
- [10] V. M. Vinokur, M. V. Feigel'man, V. B. Geshkenbein, and A. I. Larkin, *Phys. Rev. Lett.* **65**, 259 (1990).
- [11] H. Safar, P. L. Gammel, D. J. Bishop, D. B. Mitzi, and A. Kapitulnik, *Phys. Rev. Lett.* **68**, 2672 (1992).
- [12] N. V. Zavaritsky, A. V. Samoilov, and A. A. Yurgens, *Physica (Amsterdam)* **180C**, 417 (1991).
- [13] N. V. Zavaritsky, A. V. Samoilov, and A. A. Yurgens, *Physica (Amsterdam)* **169C**, 174 (1990).
- [14] Such a resistive "knee" or a "hump" may arise due either to the microscopic interlayer current [J. W. P. Hsu *et al.*, *Phys. Rev. Lett.* **67**, 2095 (1991)] or to the macroscopic redistribution of the current along the c axis as shown by R. Bursh *et al.* [*Phys. Rev. Lett.* **69**, 522 (1992)] if the current contacts are placed on one side of a sample. In both cases the knee arises because the T dependence of the resistivity along the c axis has a maximum.
- [15] V. M. Vinokur, V. B. Geshkenbein, M. V. Feigel'man, and G. Blatter (to be published).
- [16] J. Bardeen and M. J. Stephen, *Phys. Rev.* **140**, A1197 (1965).